

Osteomalacic and Hyperparathyroid Changes in Fibrous Dysplasia Of Bone: Core Biopsy Studies and Clinical Correlations

ALESSANDRO CORSI,^{1,2} MICHAEL T COLLINS,³ MARA RIMINUCCI,^{1,4} PETER GT HOWELL,^{5,6}
ALAN BOYDE,⁶ PAMELA GEHRON ROBEY,³ and PAOLO BIANCO²⁻⁴

ABSTRACT

Deposition, mineralization, and resorption of FD bone compared with unaffected bone from FD patients was investigated in iliac crest biopsy specimens from 13 patients. Compared with unaffected bone, lesional FD bone seemed to be very sensitive to the effects of PTH and renal phosphate wasting, which respectively bring about hyperparathyroid or osteomalacic changes in the lesional bone.

Introduction: Fibrous dysplasia is a genetic noninherited disease caused by activating mutations of the *GNAS1* gene, resulting in the deposition of qualitatively abnormal bone and marrow. This study was designed to learn more about the local processes of bone deposition, mineralization, and resorption within lesional fibrous dysplasia (FD) bone compared with unaffected bone of FD patients.

Methods: Histology, histomorphometry, and quantitative back-scattered electron imaging (qBSE) analysis was conducted on affected and unaffected biopsy specimens from 13 patients and correlated to markers of bone metabolism.

Results and Conclusions: There was a marked excess of unmineralized osteoid with a nonlamellar structure and a reduced mineral content in mineralized bone within FD lesions ($p < 0.001$). A negative correlation ($p = 0.05$) between osteoid thickness (O.Th) and renal tubular phosphate reabsorption (measured as TmP/GFR) was observed for lesional bone, but not for unaffected bone, in which no histological or histomorphometric evidence of osteomalacia was observed in patients with renal phosphate wasting. Histological and histomorphometric evidence of increased bone resorption was variable in lesional bone and correlated with serum levels of parathyroid hormone (PTH). Hyperparathyroidism-related histological changes were observed in fibrous dysplastic bone, but not in the unaffected bone, of patients with elevated serum PTH secondary to vitamin D deficiency. Our data indicate that, compared with unaffected bone, lesional FD bone is very sensitive to the effects of PTH and renal phosphate wasting, which, respectively, bring about hyperparathyroid or osteomalacic changes in the lesional bone. Osteomalacic and hyperparathyroid changes, which emanate from distinct metabolic derangements (which superimpose on the local effects of *GNAS1* mutations in bone), influence, in turn, the severity and type of skeletal morbidity in FD.

J Bone Miner Res 2003;18:1235–1246

Key words: fibrous dysplasia, bone pathology, bone turnover, hyperparathyroidism, osteomalacia, histology, backscattered electron imaging

INTRODUCTION

FIBROUS DYSPLASIA OF bone (FD), whether occurring as an isolated skeletal disorder or in conjunction with endocrinopathies and skin pigmentation in the McCune-Albright

syndrome (MAS), is a potentially crippling disease caused by postzygotic, activating missense mutations of the *GNAS1* gene, which encodes the α subunit of the stimulatory G protein (Gs).⁽¹⁻⁴⁾ Earlier work has shown that FD lesions develop as an expression of the impact of the causative mutations in cells of the osteogenic lineage.⁽⁵⁻⁷⁾ Mutated skeletal progenitor cells generate both the abnormal bone

The authors have no conflict of interest.

¹Dipartimento di Medicina Sperimentale, Università dell'Aquila, L'Aquila, Italy.

²Dipartimento di Medicina Sperimentale e Patologia, Università "La Sapienza," Rome, Italy.

³Craniofacial and Skeletal Diseases Branch, National Institute of Dental and Craniofacial Research, National Institutes of Health, Bethesda, Maryland, USA.

⁴Parco Scientifico Biomedico San Raffaele, Rome, Italy.

⁵Eastman Dental Institute, University College London, London, United Kingdom.

⁶Department of Anatomy and Developmental Biology, University College London, London, United Kingdom.

and the abnormal marrow, thus compounding the basic histological changes observed in FD bone.^(7,8)

Significant elevation of markers of bone turnover is commonly observed in FD patients,^(9,10) making FD a "high turnover" bone disease in a commonplace, albeit convenient, oversimplification of its nature and biology. The cellular effects of the causative mutations and their link to the clinical expressions of the disease have been only partially elucidated. Earlier work has shown, for example, that abnormal osteoblasts deposit an abnormal bone matrix in FD lesions, with characteristic changes in cell shape, bone matrix organization, pattern of expression of certain non-collagenous proteins of bone, and mineralization.^(5,8,11) The observation of a reduced mineralization of lesional bone in cases of FD has raised the possibility that a local mineralization defect may in fact represent a major determinant of skeletal morbidity in FD.^(8,12) The known occurrence of hypophosphatemic rickets/osteomalacia as a rare complication of FD^(13–15) and the more recent recognition of derangements in renal handling of phosphate as a common occurrence in FD⁽¹⁶⁾ combine to make it worthwhile to pursue a more accurate assessment of bone mineralization in FD. This study was designed to learn more about the local processes of bone deposition, mineralization, and resorption within lesional FD bone compared with unaffected bone of FD patients. Toward this goal, we studied core biopsy specimens taken from the affected or unaffected iliac crest of 13 patients with FD by histology, histomorphometry, and quantitative back-scattered electron (qBSE) imaging, and looked for potential correlations of tissue changes with relevant metabolic parameters.

MATERIALS AND METHODS

Patients

Thirteen consecutive patients who had given written informed consent were enrolled in an institutional review board (IRB)-approved study of fibrous dysplasia at the National Institutes of Health and included in this study. Seven patients (four females and three males; age range, 10–21 years; mean age, 16.2 years) showed clinical features of MAS and radiographic evidence of FD involvement of right and/or left iliac crest (group A). The other six patients (three females and three males; age range, 9–57 years; mean age, 31.6 years) showed clinical features of MAS or PFD but no radiographic evidence of FD involvement of the iliac crests (group B). A synopsis of clinical data for the patients with FD-involved or -uninvolved iliac crest is presented in Table 1.

Before biopsy, all patients had received nonsteroidal anti-inflammatory analgesics, narcotic analgesics, or a combination of the two as needed for pain. None had received bisphosphonates before the biopsy. At the time of biopsy, patient 6 (group A) was receiving methimazole, phosphorus, calcitriol, and octreotide. Patient 1 (group B) was being treated with propylthiouracil, and patient 2 (group B) was being treated with testolactone, leuprolide, and methimazole.

TABLE 1. CLINICAL DATA AND MUTATION ANALYSIS OF THE PATIENTS WITH AFFECTED (GROUP A) AND UNAFFECTED (GROUP B) ILIAC CREST

Patient	Gender/age (years)	Clinical syndrome	Mutation analysis
Group A			
1	F/16	MAS	R201C
2	M/15	MAS	R201C
3	F/20	MAS	R201C
4	M/21	MAS	R201C
5	F/18	MAS	R201H
6	F/14	MAS	R201H
7	F/10	MAS	R201C
Group B			
1	F/15	MAS	R201H
2	F/9	MAS	R201C
3	M/41	PFD	R201C
4	M/38	PFD	R201C
5	M/30	MAS	R201C
6	F/57	MAS	R201C

MAS, McCune-Albright syndrome; PFD, polyostotic fibrous dysplasia; R201C/H, cysteine or histidine substitution at the arginine 201 position of the *GNAS1* gene.

Bone biopsy

Core biopsy specimens were obtained from the FD-involved (group A) or -uninvolved (group B) iliac crests of all patients under local anesthesia. In four patients in group A (patients 1, 3, 4, and 5), tetracycline was administered before biopsy, according to the following schedule: 2 days of tetracycline (250 mg, four times per day), 10 days off drug, 2 days of tetracycline (250 mg, four times per day), 4 days off drug, and biopsy on day 5.

Mutation analysis

Mutation analysis was performed to confirm the clinical diagnosis as previously described.⁽⁸⁾ Briefly, genomic DNA (gDNA) was extracted from fresh pathological tissues or lesional stromal cell cultures by the Qiamp Tissue kit (Qiagen, Valencia, CA, USA) according to the manufacturer's instructions. A 328-bp fragment of the *GNAS1* gene (GenBank accession number M21142), including the mutation codon (R201), was amplified using the following primers: sense, 5'-GTTTCAGGACCTGCTTCGC-3' (bases 420–438); and antisense, 5'-GCAAAGCCAAGAGCGTGAG-3' (bases 728–746). A polypeptide nucleic acid (PNA) sequence complementary to the wild-type sequence (amino-terminal 5'-CGC-TGCCGTGTC-carboxy-terminal 3'; bases 436–447) was added to the reaction mixture to prevent the binding of the sense primer to the normal allele. This allowed the selective amplification and sequencing of the mutated allele. The target gDNA was amplified in a standard polymerase chain reaction (PCR) reaction mixture containing 2 μ g PNA. After 15 minutes of denaturation at 94°C, 40 cycles of amplification were performed at the following temperatures: 94°C for 30 s, 68°C for 60 s (to allow the binding of the PNA), 55°C for 30 s (to allow the binding of the sense primer), and 72°C for 60 s. The final extension was 7 minutes at 72°C. The PCR product was

TABLE 2. BIOCHEMICAL PARAMETERS FROM THE PATIENTS WITH AFFECTED (GROUP A) AND UNAFFECTED (GROUP B) ILIAC CREST

Patient	AP	OC	PYD	DPYD	PTH	25(OH)D ₃	1,25(OH) ₂ D ₃	TmP/GFR (NR) [†]
Group A								
1	306.5	225.0	354.0	95.5	3.6	50	73	2.7 (3.33–5.9)
2	4115.0	445.0	1889.5	608.0	8.5	17	90	3.9 (3.33–5.9)
3	507.5	180.0	285.0	89.8	4.4	46	64	3.1 (3.18–6.41)
4	2287.5	425.0	1574.0	421.5	5.2	25	110	2.3 (3.33–5.9)
5	223.0	140.0	119.0	31.3	2.5	105	85	3.55 (3.18–6.41)
6	1124.0	385.0	1314.5	318.5	3.8	68	113	1.65 (3.56–7.55)
7	673.5	162.5	1167.5	312.5	2.6	40	53	2.1 (3.56–7.55)
Mean ± SE	1319.6 ± 536.6	280.3 ± 50.2	957.6 ± 264.6	268.1 ± 78.8	4.6 ± 0.8	50 ± 11	84 ± 8	2.7 ± 0.3
NR*	37–116	2–15	18–40	5–14	1.0–5.1	34–101	36–144	
Group B								
1	1497.5	350.0	785.0	219.5	6.9	38	100	2.6 (3.33–5.9)
2	879.0	210.0	530.5	175.0	3.6	74	102	2.25 (3.56–7.55)
3	376.5	66.5	68.95	20.55	5.1	74	71	2.5 (3.09–4.18)
4	142.5	63.0	49.5	13.1	1.5	51	80	2.6 (3.09–4.18)
5	1900.0	260.0	828.0	211.0	7.7	28	78	2.2 (3.09–4.18)
6	402	73.0	159.5	41.85	7.4	96	85	2.6 (2.72–4.39)
Mean ± SE	866.2 ± 285.5	170.4 ± 49.5	403.5 ± 145.9	113.5 ± 40.1	5.4 ± 1.0	63 ± 10	86 ± 5	2.4 ± 0.7
NR*	37–116	2–15	18–40	5–14	1.0–5.1	34–101	36–144	

AP, alkaline phosphatase (U/liter); OC, osteocalcin ($\mu\text{g/liter}$); PTH, parathyroid hormone (pmol/liter); 25(OH)D₃, 25-hydroxyvitamin D₃ (nmol/liter); 1,25(OH)₂D₃, 1,25-di-hydroxyvitamin D₃ (pmol/liter); PYD, pyridinoline ($\mu\text{mol/mol Cr}$); DPYD, deoxypyridinoline ($\mu\text{mol/mol Cr}$).

* Adult normal range.

[†] Gender- and age-specific normal range according to Payne.⁽¹⁸⁾

purified using the Promega Wizard PCR Preps DNA Purification System (Madison, WI, USA) and sequenced using an internal (reverse) primer (5'-CCACGTCAAACATGCTGGTG-3', bases 592–611) by using dRhodamine dye-terminator cycle sequencing with AmpliTaq and the Perkin Elmer Applied Biosystem 377 Automated Sequencer.

Biochemical measures

Serum calcium, phosphorus, alkaline phosphatase (AP), osteocalcin (OC), intact parathyroid hormone (PTH), 25(OH) vitamin D₃ [25(OH)D₃], 1,25-(OH)₂ vitamin D₃ [1,25-(OH)₂D₃], and urine creatinine, calcium, phosphorus, and creatinine-normalized urinary collagen cross-links, deoxypyridinoline (DPYD) and pyridinoline (PYD), were assessed using standard techniques. 1,25(OH)₂D₃ was assayed using a radioreceptor assay (Mayo Medical Laboratories, Rochester, MN, USA). Collagen cross-linking elements, PYD and DPYD, were measured by commercially available assays using a high-pressure liquid chromatography (HPLC) technique with a 4.7% CV (Mayo Medical Laboratories). Sera measurements were performed in duplicate on specimens collected on successive days at 8:00 AM after an overnight fast while on a hospital diet. Urine measurements were performed on aliquots taken from 24-h collections. Renal phosphate handling was assessed by calculating the maximum rate of reabsorption of phosphate relative to the glomerular filtration rate (TmP/GFR), according to the technique and nomogram of Walton and Bijvoet.⁽¹⁷⁾ Except for TmP/GFR, all values were compared with those found in normal adults. Use of the adult normal range was felt to be justified based on the sexual and skeletal maturity of the patients. The TmP/GFR normal ranges were derived from those previously reported.⁽¹⁸⁾

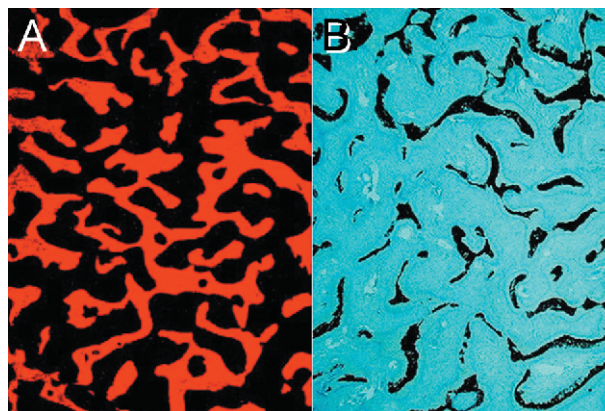


FIG. 1. Paucity of mineralized bone in FD. Patient 3, group A. (A) Paraffin and (B) MMA sections from the same biopsy. In A, the total amount of demineralized and unmineralized bone seen in a paraffin section (bone + osteoid) is visualized under fluorescence after eosin staining and digital colorization using the National Institutes of Health Image freeware. The substantial amount of total bone and the high degree of connectivity are obvious. In B, a comparable field from an MMA section after von Kossa and methylene blue staining is illustrated. A severe reduction in mineralized bone, rather than in total bone, characterizes the histology of FD.

Histology

Biopsy specimens were fixed in 4% neutral buffered formaldehyde for 2 h at 4°C. Before embedding, biopsy specimens were split lengthwise. One-half was routinely processed for paraffin embedding after decalcification with 4% EDTA in phosphate buffer (pH 7.0); the other half was

TABLE 3. RAW HISTOMORPHOMETRIC DATA FROM THE PATIENTS WITH AFFECTED (GROUP A) AND UNAFFECTED (GROUP B) ILIAC CREST

Patient	Gender/age (years)	BV/TV (%)	OS/BS (%)	O.Th μm	Oc.S/BS (%)	N.Oc/B.Pm (n/mm)
Group A						
1	F/16	38.7 (19.5–35.5)*	68.7 (17.6–46.3)*	54.0 (4.4–8.4)*	2.06 (0.42–2.94)*	1.13 (0.13–0.87)*
2	M/15	44.6 (19.5–35.5)*	70.6 (17.6–46.3)*	64.6 (4.4–8.4)*	7.52 (0.42–2.94)*	3.35 (0.13–0.87)*
3	F/20	47.0 (18.9–34.7) [†]	48.6 (4.9–23.9) [†]	74.3 (5.4–8.9) [†]	1.94 (0.51–1.89) [†]	0.90 (0.15–0.60) [†]
4	M/21	34.7 (18.9–34.7) [†]	52.2 (4.9–23.9) [†]	63.1 (5.4–8.9) [†]	3.79 (0.51–1.89) [†]	2.57 (0.15–0.60) [†]
5	F/18	47.1 (18.9–34.7) [†]	28.3 (4.9–23.9) [†]	26.0 (5.4–8.9) [†]	1.56 (0.51–1.89) [†]	0.77 (0.15–0.60) [†]
6	F/14	20.1 (19.5–35.5)*	69.9 (17.6–46.3)*	82.1 (4.4–8.4)*	2.84 (0.42–2.94)*	1.58 (0.13–0.87)*
7	F/10	40.3 (16.5–29.7) [‡]	80.2 (12.8–54.3) [‡]	83.1 (3.9–7.5) [‡]	1.13 (0.27–1.96) [‡]	0.56 (0.09–0.57) [‡]
Group B						
1	F/15	28.7 (19.5–35.5)*	22.4 (17.6–46.3)*	12.8 (4.4–8.4)*	1.03 (0.42–2.94)*	0.56 (0.13–0.87)*
2	F/9	28.2 (16.5–29.7) [‡]	8.7 (12.8–54.3) [‡]	8.0 (3.9–7.5) [‡]	1.66 (0.27–1.96) [‡]	0.56 (0.09–0.57) [‡]
3	M/41	22.0 (13.0–28.0) [§]	6.1 (4.0–39.0) [§]	11.8 (4.3–12.0) [§]	0.28 (0.0–3.1) [§]	0.04 (0.0–0.4) [§]
4	M/38	24.9 (13.0–28.0) [§]	8.0 (4.0–39.0) [§]	11.7 (4.3–12.0) [§]	0.19 (0.0–3.1) [§]	0.07 (0.0–0.4) [§]
5	M/30	26.8 (13.0–28.0) [§]	31.4 (4.0–39.0) [§]	14.4 (4.3–12.0) [§]	0.25 (0.0–3.1) [§]	0.096 (0.0–0.4) [§]
6	F/57	19.8 (15.5–28.6) [¶]	8.7 (3.8–19.3) [¶]	8.5 (6.4–13.8) [¶]	0.18 (0.0–1.57) [¶]	0.05 (0.0–0.16) [¶]

* Range from 12 (4 male, 8 female) healthy subjects, 14.0–16.9 years old.⁽²⁰⁾

[†] Range from 12 (5 male, 7 female) healthy subjects, 17.0–22.9 years old.⁽²⁰⁾

[‡] Range from 10 (8 male, 2 female) healthy subjects, 7.0–10.9 years old.⁽²⁰⁾

[§] Range from 25 healthy subjects, 19–46 years old.⁽²¹⁾

[¶] Range from 5 healthy postmenopausal females without skeletal disease, 50.0–59.0 years old (our unpublished data).

embedded undecalcified in methyl-methacrylate (MMA). Five-micron-thick sections were cut from paraffin blocks and stained with hematoxylin and eosin (H&E); 3- μm -thick sections were cut from MMA blocks and stained either with Goldner or von Kossa and methylene blue.

Histomorphometry

Histomorphometry was performed using a semiautomatic image analyzer (IAS 2000; Delta System, Rome, Italy) on MMA sections cut at intervals of 20 μm . Different parameters of bone structure, formation, and resorption were evaluated, and nomenclature and abbreviations were used as recommended by the American Society of Bone and Mineral Research.⁽¹⁹⁾ Sections stained by either von Kossa/methylene blue or Goldner's stain were used to measure bone volume/total volume (BV/TV, %), osteoid surface/bone surface (OS/BS, %), and osteoid thickness (O.Th, μm). No cut-off threshold was established for osteoid width. Osteoclast surface/bone surface (Oc.S/BS, %) and osteoclast number/bone perimeter (N.Oc/B.Pm, n/mm) were assessed on von Kossa-methylene blue-stained sections. Because in FD lesions, osteoblasts undergo characteristic shape changes and do not appear as typical cuboidal cells,^(5,11) other static parameters of bone formation based on the recognition of "active" osteoblasts, such as osteoblast surface and number, were not considered. Sections obtained from MMA blocks of tetracycline-labeled biopsy specimens were mounted unstained and viewed under fluorescence microscopy to evaluate dynamic parameters of bone formation. The results of histomorphometric analysis were reported as mean \pm SD and compared with published normative data for age-matched normal subjects^(20,21) (our unpublished data for white adults). Comparisons between groups were performed by one-way ANOVA; post hoc comparison was carried out with Schaeffe's test. Potential

correlations between biochemical markers and histomorphometric variables of bone formation and resorption were evaluated by linear regression analysis.

qBSE

qBSE analysis was conducted for patients 1–6 in group A (FD-involved iliac crest). The same MMA blocks from which histological sections were prepared and used for histology and histomorphometry were used for qBSE analysis. To this end, the blocks were diamond micromilled, coated with carbon, and studied with qBSE imaging, standardized using halogenated dimethacrylate standards as previously described (Zeiss DSM962, 0.5 nA beam current, 20 kV, 17 mm working distance, 11 mm to annular solid state BSE detector).⁽²²⁾ Samples from the iliac crest of three normal donors were analyzed in the same way and used as controls. Mean values from all patient samples and control samples were compared using one-way ANOVA. Both mean values from all patient and control samples, as well as data from each field from each sample, were analyzed using ANOVA. A Bonferroni test was used post hoc to test for differences between the six patient samples and between those samples and the control group.

RESULTS

Patients and mutation analysis

A synopsis of patient data and the mutation analysis result of the patients with FD-involved or -uninvolved iliac crest are shown in Table 1. In all patients of this series, activating mutations of the *GNAS1* gene (R201C in 10 and R201H in 3 patients) were demonstrated, thus confirming the clinicopathologic diagnosis of PFD or MAS.

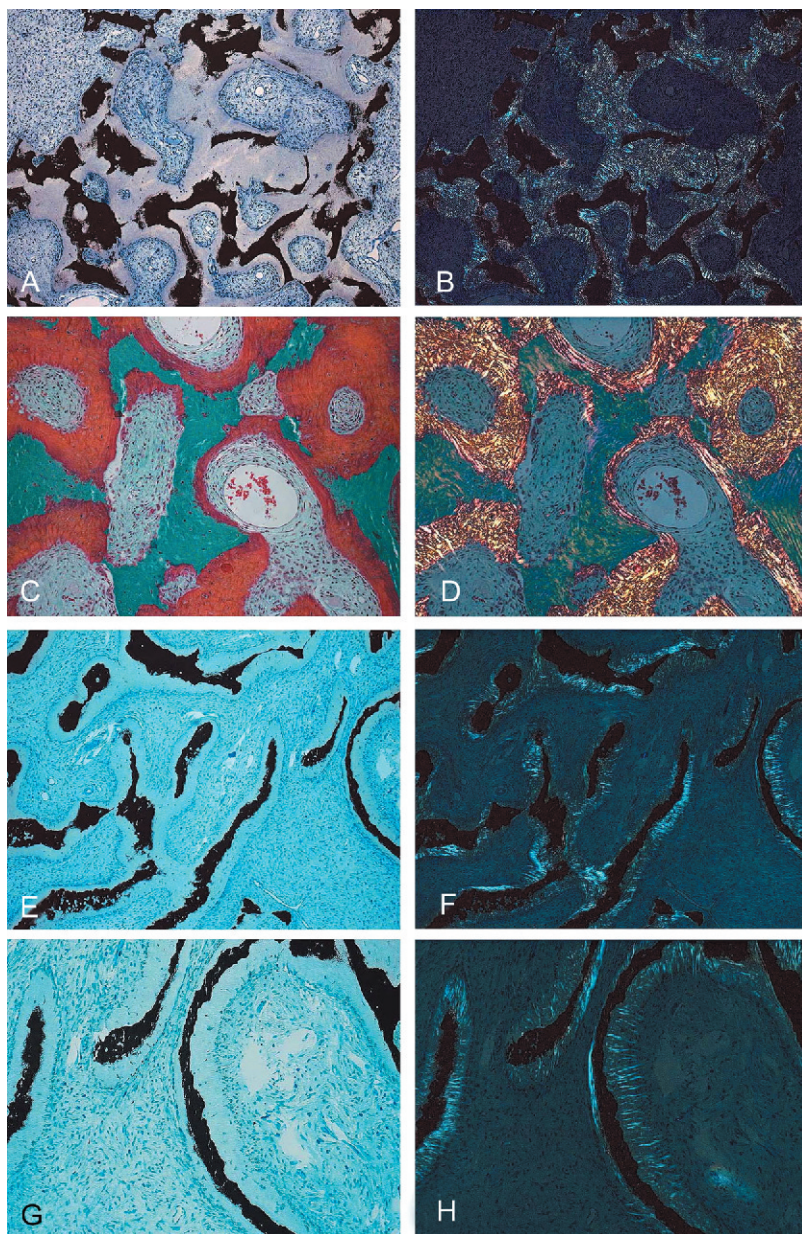


FIG. 2. Nonlamellar structure of the excess osteoid in FD bone. (A–D) Patient 3, group A. (A and C) Transmitted and (B and D) polarized light microscopy of the same fields of MMA sections stained with (A and B) von Kossa/methylene blue or (C and D) Goldner's stain. The excess of osteoid and its woven texture are obvious. (E–H) Patient 1, group A. Collagen bundles running perpendicular to the trabecular surface (i.e., Sharpey fibers) are evident in the lesional osteoid.

Biochemical analysis

Biochemical data are summarized in Table 2. In all patients, serum levels of calcium and phosphorus were within the normal range. In contrast, levels of AP, OC, and PYD were notably increased. Levels of DPYD were increased in all patients except one (patient 4, group B). Serum PTH levels were elevated in two patients in group A (patients 2 and 4) and in three patients in group B (patients 1, 5, and 6). In three of them (patients 2 and 4 in group A and patient 5 in group B), the serum concentration of 25(OH)D₃ was reduced. In patient 1 of group B, 25(OH)D₃ was at the lower limit, and in patient 6 of group B, the hyperparathyroidism was primary (parathyroid adenoma). Compared with age- and gender-matched control values, TmP/GFR was reduced

in five patients in group A (patients 1, 3, 4, 6, and 7) and in all patients in group B.

Mineralization defect in FD bone

Analysis of MMA sections stained with either von Kossa or Goldner stains revealed wide and thick osteoid seams in all FD-involved iliac crest biopsy specimens (group A). The marked paucity of mineralized bone relative to the total amount of bone and osteoid in the abnormal trabeculae of FD bone could be easily appreciated by direct comparison of H&E-stained paraffin sections, with von Kossa stained MMA sections prepared from the same biopsy in each case (Fig. 1). The large amount of unmineralized bone in FD-involved iliac crests was also reflected in normal or higher

than normal values of total bone volume (BV/TV%) on histomorphometric evaluation (Table 3), because for this purpose, we made no distinction between osteoid and bone, the total of both being the "bone" volume fraction.

Analysis of MMA sections under polarized light revealed either a typical woven bone pattern or a peculiar "Sharpey fiber" texture of the excess osteoid, whereas a lamellar structure was never observed (Fig. 2).

Measurement of osteoid surfaces and thickness (OS/BS, O.Th) confirmed the marked increase in osteoid in FD bone compared with normative values for normal bone (Table 3). In the four patients who had received tetracycline, dual labels could not be observed (Figs. 3A and 3B). Hence, the mineral apposition rate (MAR) was zero and the mineralization lag time (Mlt) was infinite, confirming the occurrence of a genuine mineralization defect in FD bone.

Values of OS/BS and O.Th recorded for the FD bone (group A) did not correlate with biochemical markers of bone formation. However, they did show an inverse correlation with renal tubular phosphate reabsorption (TmP/GFR; $r^2 = 0.56$, $p = 0.05$) as shown in Fig. 3C.

Figure 4 shows comparable grayscale BSE image fields, one from each of the group A patient biopsy specimens. It has to be remembered that the BSE images here only show the mineralized bone matrix and that unmineralized matrix (osteoid) and fibrous tissue cannot be distinguished from pure MMA. The order of presentation selected for these panels on this plate is based on the mean degree of mineralization of that bone tissue that is mineralized. It is important to note that this sequence is inverse to that of the osteoid volume fraction, that is, not only is the mineralized bone less well mineralized but also less of it is mineralized, the two factors compounding to produce the reduction in net mineral concentration. These gray scale images show a range of histological characters, ranging from those of typical woven bone (note the clustering of large osteocytic lacunar spaces and/or perilacunar mineralization deficit in Figs. 4A–4C) to more regular bone with widely and regularly separated osteocytic lacunae (Figs. 4E and 4F).

We determined whether the degree of mineralization attained by the mineralized FD bone (as measured by light microscopy of von Kossa–stained sections) was per se normal, increased or decreased with respect to age-matched normal controls by quantitative analysis of the BSE data (qBSE; Figs. 5 and 6). We used a histogram correction procedure that adjusts the gray level found for a monobrominated standard to 0 and that for a monoiodinated standard to 255.⁽²²⁾ The qBSE images show only mineralized bone matrix, because unmineralized matrix (osteoid) and pure MMA lie at or below zero. The eight color range look-up table allows easy matching of regions by degree of mineralization; any finer division gives rise to too great a complexity. Figures 5A–5E show larger fields of view, but from the same cases as in Figs. 4A–4E, respectively. Figure 5F shows a typical field from a 20.9-year-old male control biopsy. Careful study of the color scheme and the inset histograms in each image show the lower mineral concentration in the more severely affected FD cases, which again, are those with the most "osteoid"; however, a different parameter-mineral concentration in bone per se is being

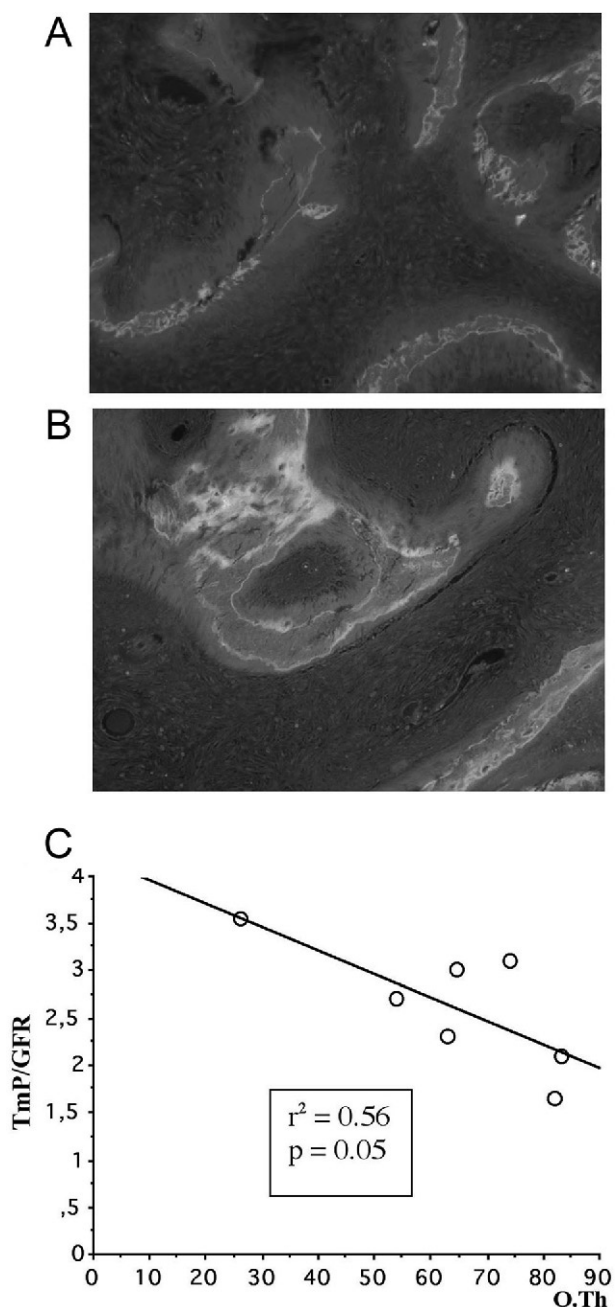


FIG. 3. (A and B) Representative fluorescence images from the FD-involved iliac crest biopsy specimens (A, patient 3; B, patient 1). Note the absence of dual labels in A and B, and the smeared pattern of fluorescence in B. (C) Inverse correlation between the osteoid thickness (O.Th) measured in FD-involved iliac crests (group A) and renal tubular phosphate reabsorption (TmP/GFR).

demonstrated here. The conclusion that the degree of mineralization of the mineralized bone matrix in FD bone was substantially lower than in age-matched reference cases was confirmed by statistical analysis ($p < 0.001$; Figs. 6A and 6B).

Analysis of iliac biopsy specimens taken from the uninvolved iliac crest of FD patients (group B) did not disclose

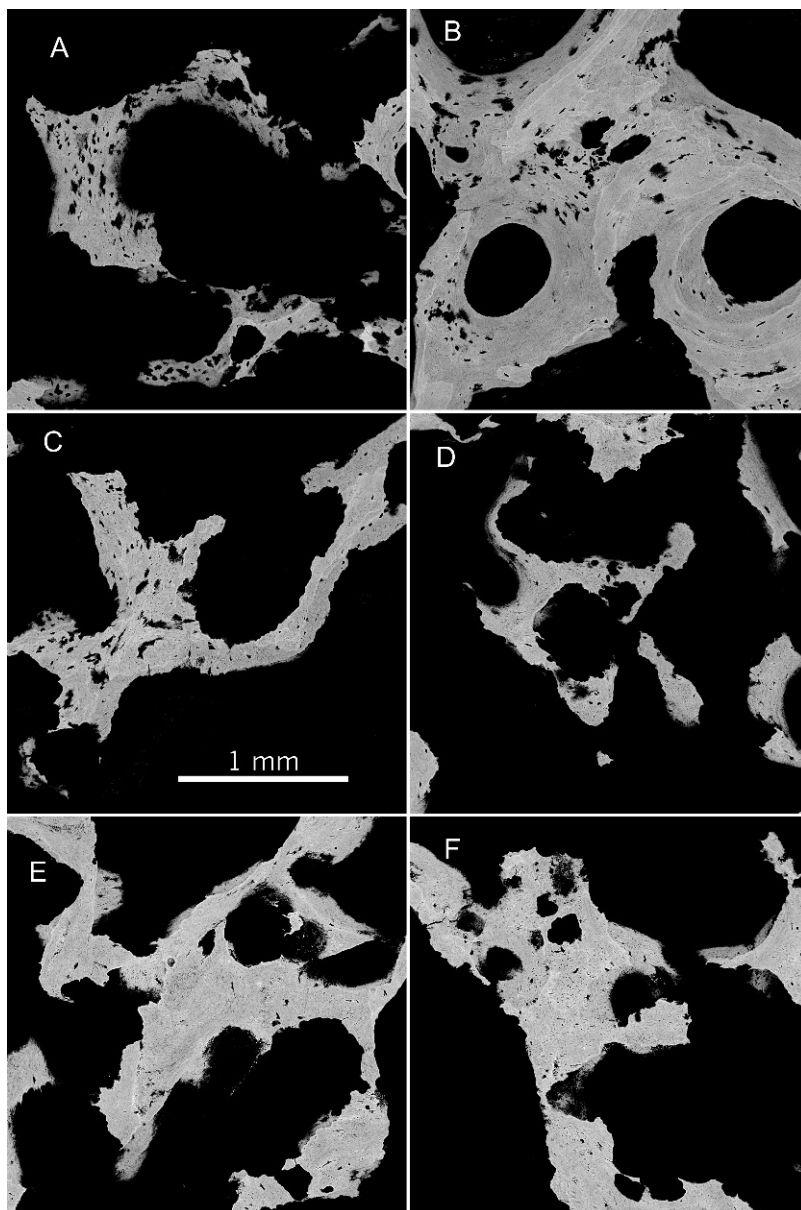


FIG. 4. Gray scale qBSE images, 2048 pixels wide and high, 1.782 mm wide and high, scale marker in C. (A) Patient 2, (B) patient 5, (C) patient 1, (D) patient 4, (E) patient 3, and (F) patient 6. (A–F) Images are ranked in ascending order of the mean mineral concentration within mineralized bone found in each case. The images show a range of BSE morphologies for bone from typical woven bone (observe the large clustering of large osteocytic lacunar spaces and/or perilacunar mineralization deficit in A–C), to more mature bone, recognized by the more widely and regularly separated osteocytic lacunae (E and F). Note that BSE imaging, as exemplified here, shows only the mineralized bone matrix; unmineralized matrix (osteoid) remains indistinguishable from pure MMA after the histogram correction procedure, which adjusts the gray level found for the monobrominated standard to 0 (and that for the monoiodinated standard to 255).

any prominent excess of osteoid. BV/TV% was within the normal range in all cases, and OS/BS was not increased in any patient in group B (Table 3). A slight increase in O.Th was recorded for three patients in group B (patients 1, 2, and 5; Table 3). Values of OS/BS and O.Th recorded for the non-FD bone (group B) did not correlate either with biochemical markers of bone formation or with renal tubular phosphate reabsorption (TmP/GFR; data not shown). Values of OS/BS and O.Th recorded for the FD bone (group A) were significantly higher than those recorded for the uninvolved bone (group B; Table 4).

Bone resorption in FD bone

Histological evidence of osteoclastic bone resorption was markedly variable in biopsy specimens taken from FD bone (group A). In two patients (patients 2 and 4), histological

evidence of intense bone resorption was much more obvious than in the remaining cases. In these two patients, tunneling resorption, formation of solid clusters of multinuclear and mononuclear osteoclasts, and osteoclasts directly apposed to osteoid were striking findings (Fig. 7). The overall histological picture observed in these cases was in sharp contrast with the picture observed in cases with a predominant osteomalacic pattern and allowed us to predict an associated hyperparathyroid state a priori, which was confirmed by measurement of serum PTH.

Histomorphometric assessment of osteoclast number (N.Oc/B.Pm) in FD bone (group A) yielded higher values in six patients (patients 1–6) compared with normative data and particularly high values in the two hyperparathyroid patients (patients 2 and 4; Table 3). In contrast, Oc.S/BS was notably elevated only in the two hyperparathyroid

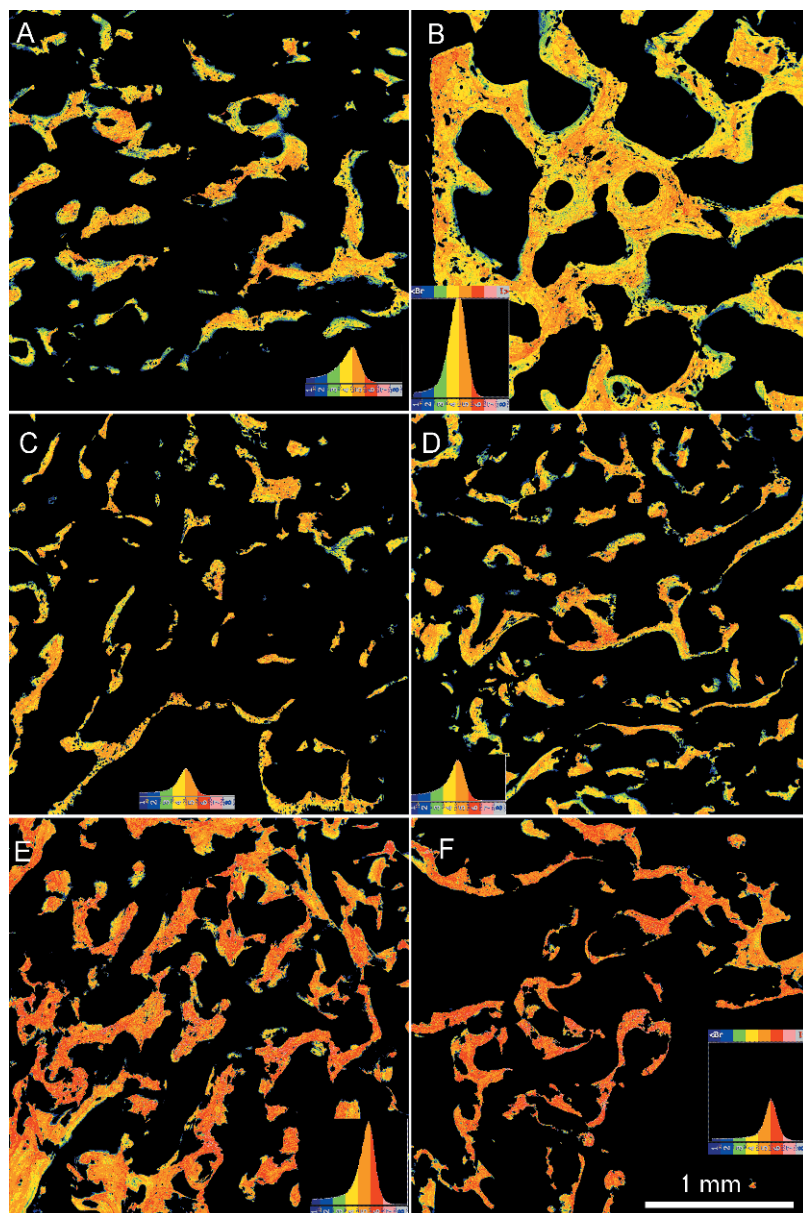


FIG. 5. Eight class pseudocolor scale qBSE images, each showing a field 2.7 mm wide and high (1 mm scale marker at bottom). (A) Patient 2, (B) patient 5, (C) patient 1, (D) patient 4, (E) patient 3, and (F) patient 6. (A–E) Images are ranked in ascending order of the mean mineral concentration within mineralized bone found in each case. Inset in each image is the histogram of mineral concentration gray scale values after the histogram correction procedure, which adjusts the gray level, found for the monobrominated standard to 0 and that for the monoiodinated standard to 255. These histograms have the same vertical scale, except that for the control case in F where this is scaled to two-thirds. Again, these images show only the mineralized bone matrix; unmineralized matrix (osteoid) and fibrous tissue are indistinguishable from MMA.

patients. A significant correlation was observed between either of these histomorphometric indices of bone resorption measured in FD bone and serum levels of PTH (Fig. 8). Likewise, significant correlations between either histomorphometric index of bone resorption in FD bone and urinary DPYD were also observed (Fig. 8).

Values of N.Oc/B.Pm and Oc.S/BS measured in the non-involved iliac crest of FD patients (group B) were in the normal range and significantly lower than those measured in the FD-involved iliac crests (group A; Table 4). They did not correlate either with serum levels of PTH or with biochemical markers of bone resorption (data not shown). Interestingly, overt histological changes of hyperparathyroidism were not observed in the uninvolved iliac crest of the three patients with elevated serum PTH in group B (patients 1, 5, and 6).

DISCUSSION

Biochemical markers of bone formation and resorption are usually elevated in patients with FD.^(9,10,12) Fibrous dysplasia of bone is therefore commonly referred to as a “high turnover” bone disease. However, aspects of bone formation and resorption within the abnormal FD bone that may be unique to the disease have received little attention. Until recently, for example, the statement that FD bone is formed “without the intervention of osteoblasts” was commonplace in textbooks. This was corrected by the recognition that osteoblasts of an abnormal and elusive shape deposit FD bone.⁽¹¹⁾ Likewise, it has only recently been recognized that the “fibroblastic” cells accumulating within the marrow space in FD in fact bear many kinships to osteoprogenitor stromal cells.^(5,11) In the present study,

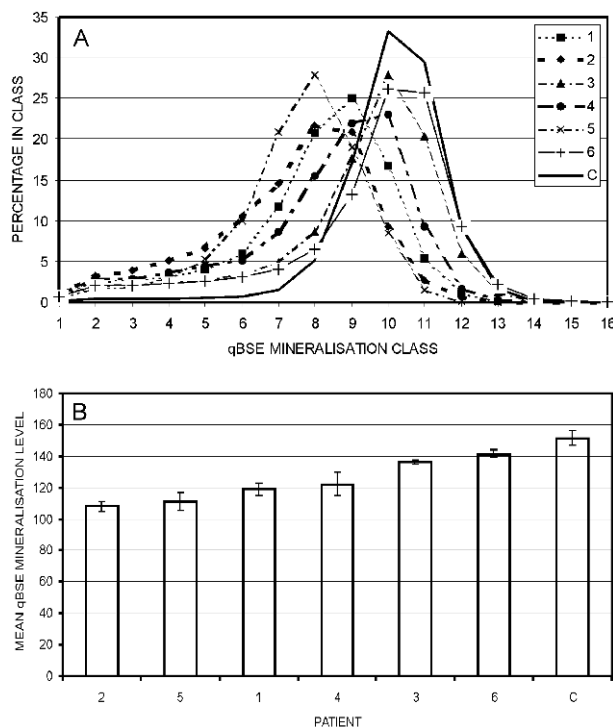


FIG. 6. (A and B) qBSE results for patients (FD-involved iliac crests) and controls. (A) Gray levels, representing the mineral concentrations, were sorted into 16 classes covering the range of values between the gray level found for the monobrominated standard, adjusted to 0, and that for the monoiodinated standard, adjusted to 255. Note the shift to the left in all affected cases. (B) The ANOVA showed that there was a significant difference between the group A patients and the normal donors ($p < 0.001$), and the post hoc tests showed that all six from group A were significantly different from the group B ($p < 0.05$).

methodological approaches suited for the histological assessment of bone metabolism have been applied to the investigation of bone turnover in FD.

Our data confirm and extend previous observations⁽⁸⁾ indicating that a significant mineralization deficit is common within FD bone and that this may indeed be considered, by standard criteria, a form of localized osteomalacia. Osteoid surfaces and thickness, two conventional light microscopic indices of osteomalacia, are markedly increased in FD bone, and dual labels are not observed in FD bone after administration of tetracycline. It should also be stressed that at variance with other instances of osteomalacia, the excess osteoid accumulating in FD never exhibits a lamellar internal structure and consists primarily of unmineralized woven bone matrix. Woven bone has a relatively lower collagen content compared with lamellar bone and a relatively higher non-collagenous protein (and water) content.^(12,23,24) This explains why woven bone that forms under physiological conditions (i.e., at early stages of bone development) mineralizes to a higher degree than mature lamellar bone. In light of this, the finding that *woven* osteoid accumulates in FD may be taken to signify an even greater impairment in mineralization compared with other instances of osteomalacia. By means of qBSE analysis, we have also shown that not only does osteoid accumulate in FD bone,

but also mineralized bone proper attains only a relatively low mineral concentration. This can hardly be interpreted as a nonspecific feature of "immaturity" of a genetically abnormal bone or as a mere consequence of an altered rate of turnover. Bone from children with osteogenesis imperfecta, which undergoes rapid remodeling, in fact attains a higher degree of mineralization compared with normals, consistent with a relative reduction in collagen content in its matrix.⁽²²⁾ Thus, qBSE data provide further evidence for a specific tendency of the bone matrix deposited within FD to remain un- or undermineralized.

The clinical implications of an inherent mineralization defect in FD bone are obvious. The abnormal compliance conveyed by a reduced mineral content in FD bone explains the tendency of affected bones to bend and deform. The mechanisms underlying osteomalacia in FD, however, have not been fully elucidated. Both intrinsic and extrinsic determinants may affect the ultimate ability of lesional FD bone to mineralize. For example, earlier immunohistological and in situ hybridization studies revealed a distinct profile of matrix protein expression in FD bone.⁽⁵⁾ An abnormal profile of non-collagenous proteins in the FD bone matrix may well contribute to an abnormal pattern of mineralization. On the other hand, the production within FD lesions of humoral factors capable of promoting renal phosphate loss and hypophosphatemia⁽²⁵⁻²⁸⁾ has been postulated as an additional or alternative mechanism.^(8,16) Severity and persistence of renal phosphate loss over time may be important in determining hypophosphatemia in those FD patients in which it does in fact occur.⁽¹⁶⁾ In the present series, none of the patients were hypophosphatemic, although most exhibited some degree of renal phosphate wasting as assessed by measuring TmP/GFR. While none of the patients with reduced TmP/GFR showed osteomalacic changes in the non-affected bone, a negative correlation of borderline significance ($p = 0.05$) was observed between O.Th (a histomorphometric index of osteomalacia) within FD bone and TmP/GFR. We take these data to indicate that an enhanced phosphate loss in the presence of normal levels of phosphatemia may affect FD bone and normal bone differentially, causing or enhancing a mineralization impairment in the former, while leaving the latter relatively unaffected. Alternately, an inherent, lesion-specific mechanism may impair mineralization in FD bone or interplay with systemic factors in producing a lesion-restricted mineralization deficit. In either case, therapeutic attempts toward the normalization of phosphatemia in FD patients would be required in cases of generalized hypophosphatemic osteomalacia complicating FD⁽¹³⁻¹⁵⁾ but may remain ineffective with respect to the mineralization defect within the lesion itself.

Enhanced osteoclastic activity, reflected in high rates of bone resorption, is thought to be a common and generalized feature of FD bone. In the series presented here, biochemical markers of bone resorption were in fact elevated in all patients. We observed that serum levels of PTH greatly affect the histological expressions of bone resorption in FD bone and correlate with histomorphometric parameters thereof. This observation highlights how the histological appearance of FD lesions (and the rate of bone turnover therein) in the individual case may reflect general hormonal

TABLE 4. STATISTICAL COMPARISON BETWEEN HISTOMORPHOMETRIC STATIC PARAMETERS OF BONE FORMATION AND RESORPTION FROM FD-INVOLVED (GROUP A) AND -UNINVOLVED (GROUP B) ILIAC CREST

Variable	Group A: affected iliac crest (N = 7, mean \pm SD)	Group B: unaffected iliac crest (N = 6, mean \pm SD)	Scheffe F-test
OS/BS	59.82 \pm 17.76	14.26 \pm 10.26	50.72*
O.Th	63.93 \pm 19.74	11.22 \pm 2.49	44.02*
Oc.S/BS	2.98 \pm 2.18	0.59 \pm 0.61	6.59*
N.Oc/B.Pm	1.55 \pm 1.03	0.23 \pm 0.25	9.24*

* Significant at 95%.

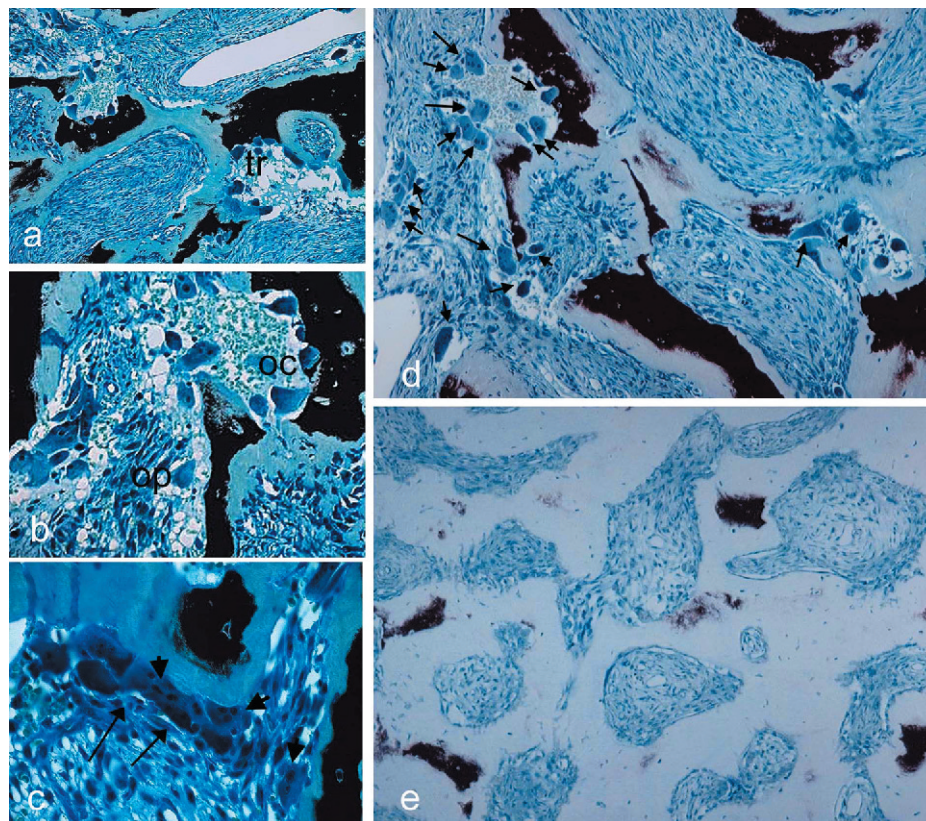


FIG. 7. Histology of FD-involved iliac crests from (a–d) two patients with secondary hyperparathyroidism and (e) one patient with severe osteomalacia and normal PTH. (a, b, and d) Patient 4 and (c) patient 2. The hyperparathyroid state was blindly predicted in both cases from histology alone, based on the unusually high numbers of multinuclear osteoclasts (oc, thick arrows in c) and osteoclast precursors (op), on the tunneling pattern of trabecular resorption (tr) and the presence of solid clusters of osteoclasts (arrows), reminiscent of microscopic brown tumors. (d and e) Low-power views of FD sections with predominant hyperparathyroid (d, patient 4) or predominant osteomalacic (e, patient 7) changes. Note the abundance of osteoclasts in d (arrows) and their absence in e. Although an excess of osteoid, which is inherent to FD, is seen in both d and e, marked osteoclastic activity is only seen in d, and the osteomalacic change is much more severe in e, where mineralized bone (black in the von Kossa stained section) is almost entirely absent. (d) FD with superimposed hyperparathyroidism. (e) FD with severe osteomalacia in the absence of hyperparathyroidism and in the absence of marked bone resorption activity.

and metabolic determinants in addition to the cell-specific effects of the causative mutation in the bone microenvironment. An FD lesion remains hormonally responsive, and the hormonal status of the patient contributes to generate diversity in FD pathology. We observed a much higher osteoclastic activity in FD bone from patients with elevated serum PTH than in those with normal levels of PTH. The observation of tunneling resorption, solid clusters of osteoclasts, and osteoclasts directly apposed on osteoid surfaces enabled

a hyperparathyroid status to be predicted blindly from histology alone in these patients. Interestingly, elevated serum PTH did not translate into hyperparathyroidism-like changes in nonaffected bone of FD patients. Thus, at least with respect to responsiveness to PTH, FD bone may in fact be more responsive than normal bone. This is fully consistent with the nature and biological effect of causative mutations in FD. A sustained and prolonged response to PTH may be envisioned to occur in the mutated cells of osteo-

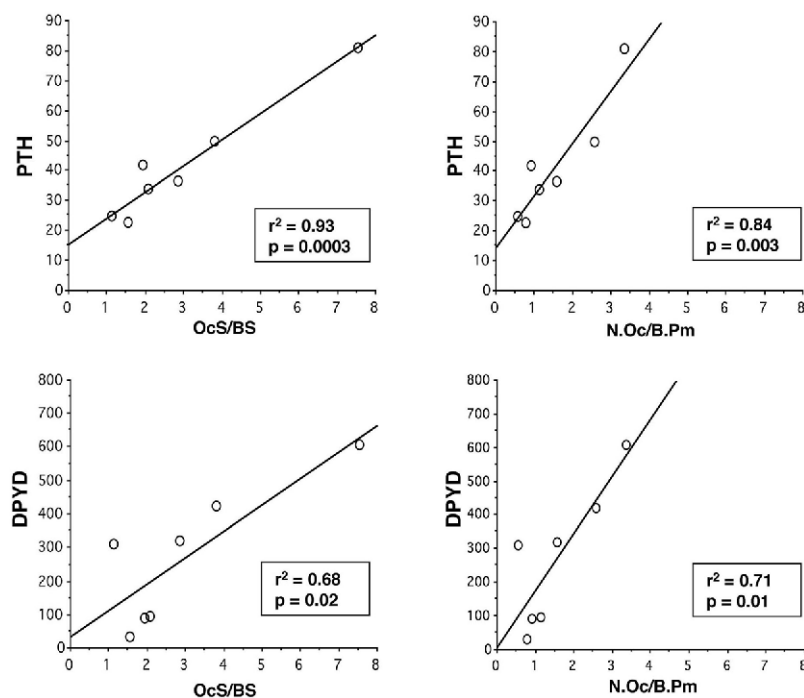


FIG. 8. Patients in group A (FD-involved iliac crest). Direct correlations of histomorphometric parameters of bone resorption (OcS/BS and N.Oc/B.Pm) measured in lesional FD bone with serum PTH (top panels) and urinary DPYD (bottom panels).

genic lineage, causing a local amplification of the biological effect of the hormone.

Taken together, our data indicate that changes in renal handling of phosphate and changes in serum levels of PTH specifically affect lesional FD bone to a greater extent than normal bone. Our observations thus concur in delineating FD bone as a site of exquisite and enhanced sensitivity to metabolic and hormonal determinants of bone turnover, and further emphasize their unique interplay with local (genetic) determinants of bone formation and resorption. Not only does FD bone remain responsive to (at least certain) hormonal inputs, but the genetic abnormality of bone cells in FD may alter their hormonal responses. A differential response of FD and non-FD bone should thus be taken into account when assessing bone metabolism in these patients. This may be relevant, for example, in considering the mechanisms for the maintenance of a normal phosphatemia in the face of phosphate leaking in some (but not all) FD patients, like those in the present series. Although, in normal subjects, the phosphaturic effect of PTH on kidney is dominant over the pro-phosphatemic effect of PTH on bone, this may not be the case in the presence of FD bone, that is, of mutated, abnormally responding, bone cells. Displacement of phosphate from bone (including removal from mineralized bone and lack of incorporation in poorly mineralizing bone) into the circulation might be greater in FD lesions than in non-FD bone in an individual patient.

When matched with metabolic assessment, the histological observations made on FD tissue seem to identify two distinct histological and metabolic profiles associated with FD. Three of seven patients exhibited a lesion histology dominated by a marked degree of osteomalacia, with markedly increased OS/BS and O.Th, moderately increased numbers of osteoclasts, but normal values of Oc.S/BS. These patients were

not hyperparathyroid, had normal levels of 25(OH)D₃, low or low-normal 1,25(OH)₂D₃, and a markedly reduced TmP/GFR despite normal phosphatemia. Two of seven patients exhibited a lesion histology dominated by marked osteoclastic activity, reflected in high values of Oc.S/BS on histomorphometric evaluation. Both patients were hyperparathyroid, with low levels of 25(OH)D₃ and normal levels of 1,25(OH)₂D₃. Another two patients in group B also had low 25(OH)D₃ and secondary hyperparathyroidism (for a total of four patients), suggesting that this profile may in turn be relatively common in association with FD/MAS. The overall frequency of phosphate wasting is estimated to be between 40% and 50% of patients with FD/MAS. The overall frequency of associated vitamin D deficiency remains to be assessed on a larger series, and its potential causes may require attention.

In summary, phosphate wasting on the one hand and vitamin D deficiency with secondary hyperparathyroidism on the other may represent distinct metabolic profiles, which associate with, and superimpose on, FD. These metabolic changes, although not caused by the presence of *GNAS1* mutations in FD bone, do affect bone turnover within FD. Once superimposed on the effects of the causative mutations in bone cells, they contribute to generate two distinct types of lesion histology (in an oversimplification, an “osteomalacic type,” noted for severe osteomalacia in the absence of markedly increased bone resorption and a “hyperparathyroid type” noted for high rates of osteoclastic resorption), which are readily distinguished from one another by histological and histomorphometric criteria.

ACKNOWLEDGMENTS

The support of Telethon Fondazione Onlus Grant E1029 (to PB) is gratefully acknowledged.

REFERENCES

1. Weinstein LS, Shenker A, Gejman PV, Merino MJ, Friedman E, Spiegel AM 1991 Activating mutations of the stimulatory G protein in the McCune-Albright syndrome. *N Engl J Med* **325**:1688–1695.
2. Schwindinger WF, Francomano CA, Levine MA 1992 Identification of a mutation in the gene encoding the alpha subunit of the stimulatory G protein of adenyl cyclase in McCune-Albright syndrome. *Proc Natl Acad Sci USA* **89**:5152–5156.
3. Alman BA, Greel DA, Wolfe HJ 1996 Activating mutations of Gs protein in monostotic fibrous lesions of bone. *J Orthop Res* **14**:311–315.
4. Shenker A, Weinstein LS, Sweet DE, Spiegel AM 1994 An activating Gs alpha mutation is present in fibrous dysplasia of bone in the McCune-Albright syndrome. *J Clin Endocrinol Metab* **79**:750–755.
5. Riminucci M, Fisher LW, Shenker A, Spiegel AM, Bianco P, Gehron Robey P 1997 Fibrous dysplasia of bone in the McCune-Albright syndrome: Abnormalities in bone formation. *Am J Pathol* **151**:1587–1600.
6. Marie PJ, de Pollak C, Chanson P, Lomri A 1997 Increased proliferation of osteoblastic cells expressing the activating Gs alpha mutation in monostotic and polyostotic fibrous dysplasia. *Am J Pathol* **150**:1059–1069.
7. Bianco P, Kuznetsov SA, Riminucci M, Fisher LW, Spiegel AM, Robey PG 1998 Reproduction of human fibrous dysplasia of bone in immunocompromised mice by transplanted mosaics of normal and Gs α -mutated skeletal progenitor cells. *J Clin Invest* **101**:1737–1744.
8. Bianco P, Riminucci M, Majolagbe A, Kuznetsov SA, Collins MT, Mankani MH, Corsi A, Bone HG, Wientroub S, Spiegel AM, Fisher LW, Robey PG 2000 Mutations of the GNAS1 gene, stromal cell dysfunction, and osteomalacic changes in non-McCune-Albright fibrous dysplasia of bone. *J Bone Miner Res* **15**:120–128.
9. Chapurlat R, Meunier PJ 1999 The nonsurgical treatment of fibrous dysplasia. *Rev Rhum Engl Ed* **66**:1–3.
10. Chapurlat R, Meunier PJ 2000 Fibrous dysplasia of bone. *Bailliere's Clin Rheum* **14**:385–398.
11. Riminucci M, Liu B, Corsi A, Shenker A, Spiegel AM, Robey PG, Bianco P 1999 The histopathology of fibrous dysplasia of bone in patients with activating mutations of the Gs alpha gene: Site-specific patterns and recurrent histological hallmarks. *J Pathol* **187**:249–258.
12. Bianco P, Gehron Robey P, Wentroub S 2003 Fibrous dysplasia. In: Glorieux FH, Pettifor J, Juppner H (eds.) *Pediatric Bone—Biology and Disease*. Academic Press, New York, NY, USA, pp. 509–539.
13. Dent CE, Gertner JM 1976 Hypophosphataemic osteomalacia in fibrous dysplasia. *Q J Med* **45**:411–420.
14. Park YK, Unni KK, Beabout JW, Hodgson SF 1994 Oncogenic osteomalacia: A clinicopathologic study of 17 bone lesions. *J Korean Med Sci* **9**:289–298.
15. Ryan WG, Nibbe AF, Schwartz TB, Ray RD 1968 Fibrous dysplasia of bone with vitamin D resistant rickets: A case study. *Metabolism* **17**:988–998.
16. Collins MT, Chebli C, Jones J, Kushner H, Consugar M, Rinaldo M, Wientroub S, Bianco P, Robey PG 2001 Renal phosphate wasting in fibrous dysplasia of bone is part of a generalized renal tubular dysfunction similar to that seen in tumor-induced osteomalacia. *J Bone Miner Res* **16**:806–813.
17. Walton RJ, Bijovet OL 1977 A simple slide-rule method for the assessment of renal tubular reabsorption of phosphate in man. *Clin Chim Acta* **81**:273–276.
18. Payne RB 1998 Renal tubular reabsorption of phosphate (TmP/GFR): Indications and interpretation. *Ann Clin Biochem* **35**:201–206.
19. Parfitt AM, Drezner MK, Glorieux FH, Kanis JA, Malluche H, Meunier PJ, Ott SM, Recker RR 1987 Bone histomorphometry: Standardization of nomenclature, symbols, and units. Report of the ASBMR Histomorphometry Nomenclature Committee. *J Bone Miner Res* **2**:595–610.
20. Glorieux FH, Travers R, Taylor A, Bowen JR, Rauch F, Norman M, Parfitt AM 2000 Normative data for iliac bone histomorphometry in growing children. *Bone* **26**:103–109.
21. Weinstein RS, Bell NH 1988 Diminished rates of bone formation in normal black adults. *N Engl J Med* **319**:1698–1701.
22. Boyde A, Travers R, Glorieux FH, Jones SJ 1999 The mineralization density of iliac crest bone from children with osteogenesis imperfecta. *Calcif Tissue Int* **64**:185–190.
23. Bianco P 1992 Structure and mineralization of bone. In: Bonucci E (ed.) *Mineralization in Biological Systems*. CRC Press, Boca Raton, FL, USA, pp. 243–268.
24. Gehron Robey P, Bianco P 2002 The cellular biology and molecular biochemistry of bone formation. In: Favus MJ (ed.) *Disorders of Bone Miner Metabolism*, 2nd ed. Raven Press, New York, NY, USA, pp. 199–226.
25. Drezner MK 2000 PHEX gene hypophosphatemia. *Kidney Int* **57**:9–18.
26. Kumar R 2000 Tumor-induced osteomalacia and the regulation of phosphate homeostasis. *Bone* **27**:333–338.
27. Rowe PS, de Zoysa PA, Dong R, Wang HR, White KE, Econs MJ, Oudet CL 2000 MEPE, a new gene expressed in bone marrow and tumors causing osteomalacia. *Genomics* **67**:54–68.
28. White KE, Evans WE, O'Riordan JL, Speer MC, Econs MJ, Lorenz-Depiereux B, Grabowski M, Meitinger T, Strom TM 2000 Autosomal dominant hypophosphataemic rickets is associated with mutations in FGF23. *Nat Genet* **26**:345–348.

Address reprint requests to:

Paolo Bianco, MD

Dipartimento di Medicina Sperimentale e Patologia

Universita "La Sapienza"

Viale Regina Elena 324

Rome 00161, Italy

E-mail: p.bianco@flashnet.it

Received in original form November 19, 2002; in revised form December 20, 2002; accepted January 10, 2003.